Special Issue

Quantifying Microvascular Abnormalities With Increasing Severity of Diabetic Retinopathy Using Optical Coherence Tomography Angiography

Peter L. Nesper,[1] Philipp K. Roberts,[1,2] Alex C. Onishi,[1] Haitao Chai,[3,4] Lei Liu,[3] Lee M. Jampol,[1] and Amani A. Fawzi[1]

[1]Department of Ophthalmology, Feinberg School of Medicine, Northwestern University, Chicago, Illinois, United States
[2]Department of Ophthalmology and Optometry, Medical University of Vienna, Vienna, Austria
[3]Department of Preventive Medicine, Feinberg School of Medicine, Northwestern University, Chicago, Illinois, United States
[4]Institute for Financial Studies, Shandong University, Jinan, China

Correspondence: Amani A. Fawzi, Department of Ophthalmology, Northwestern University, Feinberg School of Medicine, 645 N. Michigan Avenue, Suite 440, Chicago, IL 60611, USA; afawzimd@gmail.com.

PLN and PKR contributed equally to the work presented here and should therefore be regarded as equivalent authors.

Submitted: March 1, 2017
Accepted: June 10, 2017

Citation: Nesper PL, Roberts PK, Onishi AC, et al. Quantifying microvascular abnormalities with increasing severity of diabetic retinopathy using optical coherence tomography angiography. *Invest Ophthalmol Vis Sci*. 2017;58:BIO307–BIO315. DOI: 10.1167/iovs.17-21787

Purpose. We quantified retinal and choriocapillaris microvascular changes in healthy control eyes and different stages of diabetic retinopathy (DR) using optical coherence tomography angiography (OCTA).

Methods. This retrospective cross-sectional study included 137 eyes of 86 patients with different stages of DR and 44 eyes of 26 healthy age-matched controls. Participants were imaged with a commercial OCTA device (RTVue-XR Avanti). We analyzed the superficial (SCP) and deep (DCP) retinal capillary plexus, the full retina, and choriocapillaris for the following OCTA parameters: foveal avascular zone, vessel density, percent area of nonperfusion (PAN), and adjusted flow index (AFI). We adjusted for age, sex, and the correlation between eyes of the same study participant in our statistical models.

Results. All OCTA parameters showed a significant linear correlation with DR severity ($P < 0.05$) in the univariate models except for AFI measured in the SCP and these correlations remained significant after correcting for covariates. Compared to the other capillary layers, the AFI at the DCP decreased significantly with DR severity. When comparing individual disease severity groups as categories, eyes of subjects with diabetes without DR had significantly increased PAN and AFI in the SCP compared to healthy subjects ($P < 0.05$).

Conclusions. Retinal and choriocapillaris vascular nonperfusion in OCTA is correlated significantly with disease severity in eyes with DR. Higher flow in the SCP may be an early marker of diabetic microvascular changes before clinical signs of DR. The steep decline of blood flow in the DCP with increasing DR severity suggests that alterations at the DCP warrant further investigation.

Keywords: optical coherence tomography angiography, diabetic retinopathy, imaging

Diabetic retinopathy (DR) is the consequence of a systemic microangiopathy in the unique intraocular environment. Histopathology has shown that degeneration of the retinal capillary pericytes and endothelial cells are early and seemingly invariable features of DR.[1,2] The loss of these cells leads to acellular capillaries with impaired or absent perfusion.[3] The resulting ischemia causes an upregulation of angiogenic signaling molecules, including VEGF and erythropoietin,[4] which increase vascular permeability and ultimately promote proliferative diabetic retinopathy (PDR).[5] A clinical understanding of the changes at the microvascular level could provide important information regarding the perfusion status of the retina during the different stages of DR and the likelihood of developing more severe retinopathy.

Optical coherence tomography angiography (OCTA) provides a rapid, noninvasive technique to visualize the retinal and choroidal vasculature in vivo. The ability of OCTA to visualize the three-dimensional capillary layers with high resolution has allowed investigators to explore the capillary layers that are most affected in DR.[6–8] Previous qualitative studies in DR have demonstrated that OCTA is capable of delineating retinal capillary nonperfusion with better resolution than conventional fluorescein angiography.[9–11] Other studies have found decreased capillary density in patients with DR compared to healthy controls, as well as an association between reduced capillary density and worsening DR.[12,13] Furthermore, the ability of OCTA to distinguish healthy eyes from eyes with varying levels of DR severity was demonstrated through the use of an automated algorithm for measuring avascular areas in the macula.[14,15]

While the studies described provide important information regarding the use of OCTA and have furthered our understanding of the vascular changes associated with DR, they have been limited to small cohorts and comparisons between only two study groups. These previous studies also are limited by their pilot nature, which did not allow correction for patient characteristics that may confound the vascular changes.

In this larger cohort study, we studied several OCTA-based vascular parameters, including adjusted flow index (AFI), an indirect and relative measure of flow velocity. We compared the findings between four groups: healthy controls, diabetes mellitus

(DM) without DR, nonproliferative (NPDR), and PDR. To address some of the limitations in previous studies, we used a linear mixed model to correct for patient demographics. The primary outcome was the correlation of OCTA vascular abnormalities to disease severity. Based on the higher prevalence of retinal microaneurysms in the deep capillary plexus (DCP),[16] we hypothesized that the vascular changes at the level of the DCP would be correlated more significantly to disease severity compared to the superficial capillary plexus (SCP), full retinal thickness, or choriocapillaris.

Methods

This was a retrospective analysis of healthy participants and patients with diabetes recruited in the Department of Ophthalmology at Northwestern University in Chicago, Illinois between June 2015 and July 2016. The study was approved by the institutional review board of Northwestern University, followed the tenets of the Declaration of Helsinki, and was performed in accordance with Health Insurance Portability and Accountability Act regulations. Written informed consent was obtained from all participants.

Study Sample

Inclusion criteria were healthy eyes, eyes from patients with DM without DR, eyes with NPDR, or eyes with PDR based on clinical assessment by two retina specialists (A.A.F. or L.M.J.).[17] We included treatment-naïve eyes and those treated previously with intravitreal anti-VEGF agents, intravitreal triamcinolone acetonide, dexamethasone intravitreal implant, focal laser and/or panretinal photocoagulation, or pars plana vitrectomy. Only eyes that had OCTA images without significant movement or shadow artifacts, and a signal strength index (SSI) score above 50 were considered eligible.

Exclusion criteria were eyes with other retinal diseases that may confound our results. We also excluded patients with astigmatism (more than 3 diopters), high refractive error (more than 6 diopters), or cataract graded above nuclear opalescence grade three or nuclear color grade three, to avoid optical artifacts that potentially may compromise OCTA image quality. We excluded eyes with evidence of one or more large hemorrhages in the central 3×3 mm^2, but included eyes with small intraretinal hemorrhages. Electronic medical records were reviewed to extract demographic and clinical information (Table 1). Monocular best-corrected visual acuity (BCVA) was determined for all subjects using Snellen eye charts and converted to the logMAR as described previously.[18] Patients were graded as having hypertension based on review of their electronic medical records. Chronic kidney disease (CKD) stages were determined according to Kidney Disease Outcome Quality Initiative (KDOQI) guidelines with estimated glomerular filtration rates (eGFR) calculated through the Modification of Diet in Renal Disease (MDRD) Study equation with available creatinine, age, and racial information obtained from medical records. Healthy controls without creatinine testing were assumed to have CKD stage 1.

Angiographic Imaging and Image Processing

OCTA images were obtained using the RTVue-XR Avanti system (Optovue, Inc., Fremont, CA, USA) with split-spectrum amplitude-decorrelation angiography (SSADA) software.[19] This instrument has an A-scan rate of 70,000 scans per second and uses a light source centered at 840 nm and a bandwidth of 45 nm. Two consecutive B-scans (M-B frames), each containing 304 A-scans, were captured at each sampling location and SSADA was used to extract OCTA information. We obtained 3×3 mm^2 scans centered on the fovea. The SSI and foveal thickness for each image were recorded. Foveal thickness was defined as the average retinal thickness within the central 1 mm diameter ring.

En face OCT angiograms were segmented automatically using the built-in software to define the SCP, DCP, and choriocapillaris. For the SCP, the inner boundary of the en face image segment was set at 3 μm beneath the internal limiting membrane (ILM), and the outer boundary was set at 15 μm beneath the inner plexiform layer (IPL). For the DCP, the inner boundary was set at 15 μm beneath the IPL and the outer boundary was set at 70 μm beneath the IPL. For the choriocapillaris, the inner and outer boundaries were set at 31 and 59 μm beneath the RPE reference line, respectively. The retinal pigment epithelium (RPE) reference line is located at the middle of the hyperreflective RPE band on OCT. We also manually segmented an angiographic full retinal thickness slab, from 3 μm beneath the ILM to the middle of the outer nuclear layer (~90 μm beneath the IPL depending on retinal thickness).

We evaluated OCT B-scans and en face structural OCT images to determine if areas of hyporeflectivity were artifactual or real. We excluded images with significant artifactual components, such as enhanced decorrelation signal from excessive eye motion, or hyporeflectivity due to blockage of OCT signal from media opacity. We included all images with reflectivity changes on OCT due to DR pathology, such as edema or retinal hard exudates. The presence or absence of edema and retinal hard exudates was recorded.

Vessel Density

We used the built-in AngioVue Analytics software (version 2016.1.0.26) to obtain parafoveal blood vessel density for the SCP, DCP, and full retinal thickness angiograms (Fig. 1). The "parafovea" is defined as an annulus centered on the fovea with inner and outer ring diameters of 1 and 3 mm, respectively. Vessel density was reported as the percentage of the total area within the parafovea that was occupied by blood vessels. To calculate vessel density, the AngioVue Analytics software extracts a binary image of the blood vessels from the grayscale OCTA image, and then calculates the percentage of pixels occupied by blood vessels in the defined region.

Adjusted Flow Index

We then set out to establish a global threshold for each eye to distinguish vessels from background noise. We exported the SCP, DCP, full retinal thickness, and choriocapillaris angiograms into ImageJ (developed by Wayne Rasband, National Institutes of Health [NIH], Bethesda, MD, USA; available in the public domain at http://rsb.info.nih.gov/ij/index.html). On the SCP angiogram, we selected an area within the foveal avascular zone (FAZ) using a circle with a 30-pixel radius. We obtained the mean pixel intensity within the circle and repeated this three times. We took the average of the three selections as the noise level for that eye (Fig. 2). All pixels with intensities above the noise level were considered "vessels" and pixels with intensities below the noise level were considered "nonperfusion." For each of the four segmented angiograms, we calculated the AFI, a surrogate for flow index, and defined as the average decorrelation value of all pixels above the noise threshold (only "vessels") in the en face angiogram.[19,20]

Percent Area of Nonperfusion

We exported the SCP, DCP, full retinal thickness, and choriocapillaris angiograms into a custom made MATLAB

Investigative Ophthalmology & Visual Science

Table 1. Demographic and Disease-Related Patient Characteristics

	Healthy Controls	DM Without DR	NPDR	PDR	*P* Value
Patients, *n*	26	27	32	27	
Eyes, *n*	44	45	52	40	
Sex					<0.01
Female, *n* (%)	10 (38%)	20 (74%)	13 (41%)	12 (44%)	
Male, *n* (%)	16 (62%)	7 (26%)	19 (59%)	15 (56%)	
Age, y, mean ± SD	50 ± 18	57 ± 10	54 ± 12	49 ± 14	0.062
DM type					0.798
Type 1, *n* (%)	N/A	7 (26%)	7 (22%)	8 (30%)	
Type 2, *n* (%)	N/A	20 (74%)	25 (78%)	19 (70%)	
Disease duration, y, mean ± SD	N/A	11 ± 15	17 ± 12	19 ± 10	<0.01
Arterial hypertension					<0.01
Yes	6 (23%)	17 (63%)	16 (50%)	22 (81%)	
No	20 (77%)	10 (37%)	15 (47%)	4 (15%)	
Missing, *n* (%)	0 (0%)	0 (0%)	1 (3%)	1 (4%)	
CKD stage,* mean ± SD					0.197
Stage 1	21 (81%)	8 (30%)	5 (16%)	5 (19%)	
Stage 2	5 (19%)	6 (22%)	7 (22%)	6 (22%)	
Stage 3	0 (0%)	3 (11%)	5 (16%)	5 (19%)	
Stage 4	0 (0%)	1 (4%)	1 (3%)	1 (4%)	
Stage 5	0 (0%)	0 (0%)	1 (3%)	6 (22%)	
Missing		9 (33%)	13 (41%)	4 (15%)	
HbA1c, mean ± SD	N/A	7.50 (± 1.60)	8.65 (± 1.83)	8.20 (± 2.26)	0.08
Missing, *n* (%)		4 (15%)	7 (22%)	6 (22%)	
Visual acuity, logMAR; mean (± SD)	0.03 (± 0.07)	0.08 (± 0.10)	0.08 (± 0.11)	0.20 (± 0.25)	<0.01
SSI, mean ± SD	67 ± 7	68 ± 7	66 ± 7	64 ± 8	0.172
Foveal retinal thickness, mean ± SD, μm	321 ± 13	313 ± 15	314 ± 31	302 ± 35	<0.01
Lens status					
Clear lens	26 (59%)	20 (44%)	19 (37%)	11 (28%)	
Cataract	12 (27%)	24 (53%)	26 (50%)	23 (58%)	
Pseudophakic	6 (14%)	1 (2%)	7 (14%)	6 (15%)	
Treatment					
Anti-VEGF	N/A	0 (0%)	4 (8%)	3 (8%)	
Dexamethasone intravitreal implant	N/A	0 (0%)	0 (0%)	1 (3%)	
IVTA	N/A	1 (2%)	0 (0%)	0 (0%)	
Focal laser	N/A	0 (0%)	3 (6%)	6 (15%)	
PRP	N/A	0 (0%)	1 (2%)	30 (75%)	
PPV	N/A	0 (0%)	0 (0%)	3 (8%)	
No treatment	N/A	44 (98%)	44 (85%)	9 (23%)	

HbA1c, Hemoglobin A1c; IVTA, intravitreal triamcinolone acetonide; PRP, panretinal photocoagulation; PPV, pars plana vitrectomy; *P* Value, Pearson χ^2 or Kruskal Wallis comparison between groups.

* The *P* value is only representative for the difference between the patient groups. The healthy control group was not included.

(MathWorks, Inc., Natick, MA, USA) code. This software automatically calculated the percentage of pixels in each angiogram below the noise level, or "percent area of nonperfusion" (PAN).[21] In this study, we used PAN as a metric of the extent of nonperfusion in each vascular layer (Fig. 2).

Statistical Analysis

For statistical analysis, we used IBM SPSS statistics version 21 (IBM SPSS Statistics; IBM Corporation, Chicago, IL, USA) and R (R 3.0.2 [64-bit], The R Foundation). Shapiro Wilk tests were used to determine if demographic data were distributed normally. The differences between the groups then were assessed with either Pearson χ^2 or Kruskal-Wallis tests, based on their distribution. Spearman and Pearson correlation coefficients were used to examine nonlinear and linear correlations between the OCTA parameters and DR severity groups (healthy controls, DM without DR, NPDR, PDR).

Second, we used linear mixed effects models for the FAZ, vessel density, PAN, and AFI, adjusting for the demographic factors sex and age. In these models, we also included random effects for the correlation of two eyes from the same participants on the OCTA outcome measures, as most participants had bilateral imaging. We analyzed the data using DR severity groups defined as either a continuous or categorical variable. The models were fitted in R using the lme4 package (available in the public domain at https://cran.r-project.org/web/packages/lme4/index.html).

Third, we plotted the regression lines for FAZ, vessel density, PAN, and AFI of the SCP, DCP, full retina, and choriocapillaris for DR severity groups for a straightforward comparison. A *P* value of 0.05 was considered statistically significant.

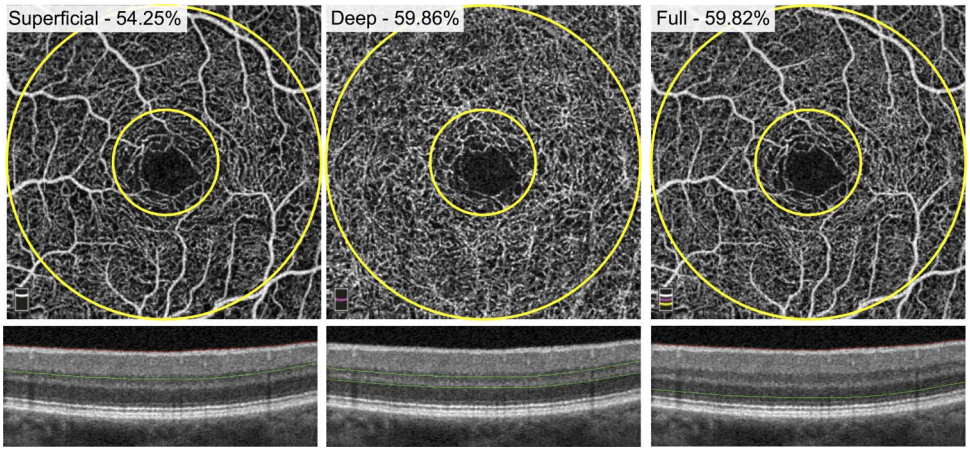

Figure 1. Parafoveal retinal vessel density measurement. En face OCTA images of the SCP (*left*), DCP (*middle*), and full retinal thickness angiogram (*right*) of a healthy patient. *Green* segmentation boundaries are shown below on cross-sectional OCT. The parafovea is defined as the area between the two *yellow circles* on each angiogram (diameters of 1 and 3 mm). The density measurements are reported as a percentage of total vessels occupying the parafovea for each layer.

Finally, in addition to adjusting for sex, age, and the correlation between two eyes from the same subject in the linear mixed effects models, we also adjusted for hypertension, which was significantly different between disease severity groups in the univariate analysis ($P < 0.01$; Table 1). We analyzed the data using DR severity groups defined as either a continuous or categorical variable.

Results

Of a total of 194 eyes imaged for this study, 13 were excluded due to SSI below 50 or significant artifacts on OCTA images, leaving a total of 181 eyes of 112 study participants (86 patients with diabetes, 26 healthy age-matched controls). The study included 44 healthy control eyes, 45 eyes of patients

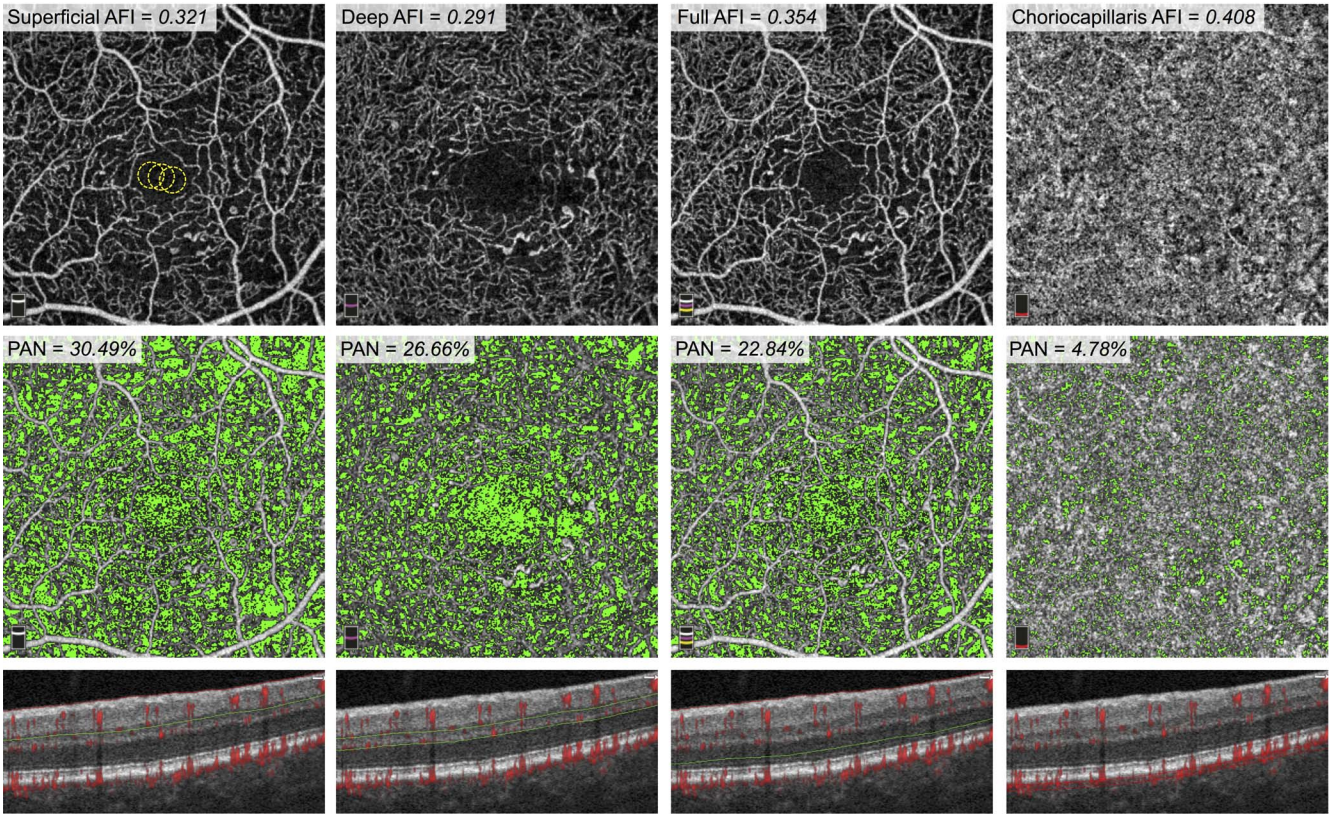

Figure 2. AFI and PAN Measurements in an eye with NPDR. *Top Row*: En face OCTA of the SCP (*left*), DCP (*middle-left*), full retinal thickness (*middle-right*), and choriocapillaris (*right*). The FAZ of the SCP shows three *yellow circles* (30-pixel radii), which were the areas used to calculate the noise threshold for this eye. The AFI, or average decorrelation value above this threshold, is reported for each layer. *Middle Row*: Areas of nonperfusion, defined as pixels with values below the noise threshold, are shown here in *green* and reported as PAN. *Bottom Row*: Cross-sectional OCT with *red* flow overlay representing decorrelation. *Green* and *red* segmentation boundaries are shown for each capillary layer.

Investigative Ophthalmology & Visual Science

Table 2. Univariate Correlations Between OCTA Parameters and Severity of DR

Outcome Measures	Healthy Controls, $n = 44$	DM Without DR, $n = 45$	NPDR, $n = 52$	PDR, $n = 40$	Spearman R Value	Spearman P Value	Pearson R Value	Pearson P Value
FAZ, mean ± SD, mm^2								
SCP	0.269 ± 0.086	0.309 ± 0.140	0.356 ± 0.207	0.493 ± 0.238	0.406	<0.01*	0.396	<0.01*
Full retina	0.273 ± 0.082	0.313 ± 0.141	0.353 ± 0.199	0.491 ± 0.232	0.394	<0.01*	0.391	<0.01*
Vessel density, mean ± SD, %								
SCP	53.59 ± 3.18	53.02 ± 3.11	46.59 ± 4.88	43.43 ± 3.83	−0.738	<0.01*	−0.708	<0.01*
DCP	60.82 ± 2.44	59.14 ± 2.80	53.76 ± 4.63	49.73 ± 3.66	−0.798	<0.01*	−0.760	<0.01*
Full	57.74 ± 3.25	57.28 ± 3.24	51.23 ± 5.16	47.47 ± 4.40	−0.708	<0.01*	−0.685	<0.01*
PAN, mean ± SD, %								
SCP	13.12 ± 3.17	15.73 ± 5.49	22.42 ± 6.91	26.99 ± 6.87	0.702	<0.01*	0.669	<0.01*
DCP	9.31 ± 2.91	11.67 ± 4.49	17.84 ± 6.17	24.67 ± 8.53	0.732	<0.01*	0.691	<0.01*
Full	9.19 ± 2.62	11.34 ± 3.87	16.16 ± 5.25	21.80 ± 6.41	0.711	<0.01*	0.694	<0.01*
CC	2.53 ± 0.69	3.39 ± 1.37	3.37 ± 1.08	4.40 ± 1.68	0.414	<0.01*	0.431	<0.01*
AFI, mean ± SD								
SCP	0.281 ± 0.028	0.291 ± 0.031	0.276 ± 0.037	0.271 ± 0.038	−0.149	0.05†	−0.143	0.06
DCP	0.298 ± 0.029	0.299 ± 0.035	0.265 ± 0.043	0.258 ± 0.040	−0.411	<0.01*	−0.409	<0.01*
Full	0.311 ± 0.029	0.321 ± 0.032	0.299 ± 0.039	0.296 ± 0.038	−0.212	<0.01*	−0.203	<0.01*
CC	0.393 ± 0.020	0.392 ± 0.022	0.382 ± 0.026	0.380 ± 0.027	−0.205	<0.01*	−0.222	<0.01*

* Correlation is significant at the 0.01 level (2-tailed).
† Correlation is significant at the 0.05 level (2-tailed).

with DM without DR, 52 eyes with NPDR, and 40 eyes with PDR. The overall demographic and disease-related characteristics are reported in Table 1.

Table 2 shows the average FAZ area, vessel density, PAN, and AFI for applicable retinal layers for each group (healthy control, DM without DR, NPDR, PDR). In Spearman and Pearson correlation analyses, we observed significant correlations between DR severity and all of the evaluated OCTA parameters except for the AFI measured in the SCP (Table 2). The FAZ area measured at the SCP and full retina increased significantly with DR severity. Retinal vessel density measured at the SCP, DCP, and full retina decreased significantly with DR severity. PAN measured in the SCP, DCP, full retina, and choriocapillaris increased significantly with increasing severity of DR (Table 2). Mean AFI in the DCP, full retina, and choriocapillaris was correlated significantly negatively with DR severity (Table 2). A mild negative trend also was seen for AFI in the SCP, but this correlation was not significant.

Figure 3 shows a representative sample of full retinal vessel density and PAN measurements with increasing DR severity.

The Spearman correlation between DR severity and either vessel density or PAN in SCP, DCP, or full retina was above ±0.7 and, therefore, was considered strong (Table 2). The Pearson correlation coefficients for SCP, DCP, and full retinal vessel density (range, $R = -0.760$ to -0.685) and PAN (range, $R = 0.669$–0.694) were close to ±0.7 as well, indicating a strong correlation with DR severity. PAN measured for the choriocapillaris showed a lower correlation with disease severity ($R = 0.414$; $P < 0.01$ and $R = 0.431$; $P < 0.01$, respectively) than the SCP, DCP, and full retina.

In the mixed effects model we adjusted for sex and age and the correlation between the two eyes of the same participant. Table 3 summarizes the outcomes of this model with DR severity groups defined as either continuous (to test for a linear correlation) or categorical (to test for a difference between each DR severity group and the healthy controls) variables, respectively.

When DR severity groups were defined as a continuous variable, all evaluated OCTA parameters, except AFI in the SCP, showed a significant linear correlation with DR severity (Table 3).

When DR severity groups were defined as categorical variables, we observed significant differences between healthy controls and the DM without DR group for PAN in the SCP, full retina, and choriocapillaris and for the AFI in the SCP. There were significant differences between the healthy control group and the NPDR group for FAZ in the SCP and for vessel density and PAN in all capillary layers, as well as the AFI in the DCP. We also observed significant differences between healthy controls and the PDR group in all evaluated OCTA parameters except for AFI measured in the SCP (Table 3).

In the third model, where we compared fitted regression lines for DR severity, we found no significant difference between the FAZ area in the SCP and full retina or retinal vessel density comparing the SCP, DCP, and full retina. The fitted regression line for the correlation between choriocapillaris PAN deviated significantly from the regression lines for the other layers (estimate $= -4.287$, $P < 2.16\ e^{-16}$; Fig. 4). Finally, the fitted regression line for AFI at the DCP deviated significantly from all the other layers (estimate $= -1.100\ e^{-02}$, $P = 6.01\ e^{-07}$; Fig. 4).

In the mixed effects models adjusted for hypertension as well as sex, age, and two eyes of the same participant, the trends were consistent with those found in the analysis without controlling for hypertension and the results were largely unchanged, with the following exceptions. When DR severity was defined as a continuous variable, the AFI in the full retina was no longer significant after correcting for hypertension, though the trend still was negative (estimate, $-5.053\ e^{-03}$; $P = 0.07$). Interestingly and in line with this result, when DR severity groups were compared individually, the full retina AFI became statistically significantly higher in DM without DR compared to healthy controls (estimate, $1.890\ e^{-02}$; $P = 0.02$), while the lower AFI in PDR compared to healthy controls lost significance (estimate, $-6.883\ e^{-03}$; $P = 0.44$). Overall, the full retina AFI now mirrored the findings in the SCP AFI (controlling for hypertension), further supporting the validity of the SCP AFI results.

Investigative Ophthalmology & Visual Science

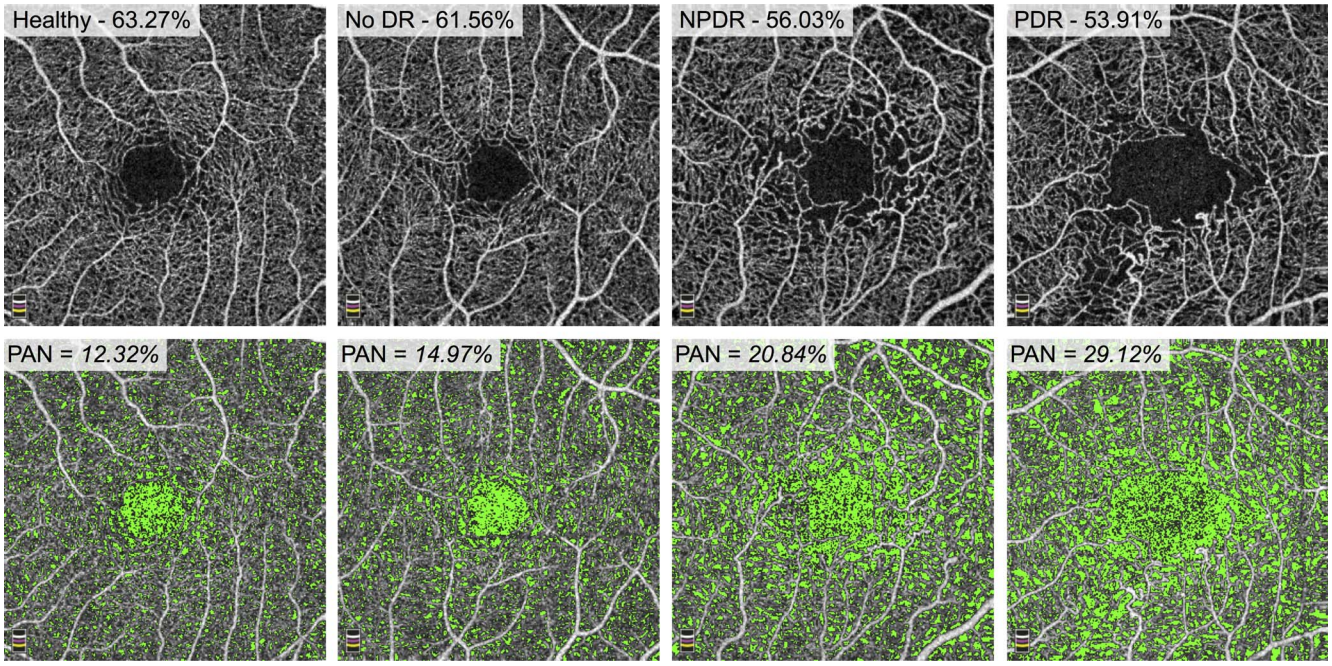

Figure 3. Vessel density decreases and PAN increases with increasing disease severity. Top Row: En face OCTA of full retinal thickness angiograms for a healthy patient (*left*), a patient with diabetes without DR (*middle left*), a patient with NPDR (*middle right*), and PDR (*right*). The parafoveal vessel density is reported as a percentage and decreases from *left* to *right*. *Bottom Row*: Areas of nonperfusion are shown in *green*. PAN is reported as a percentage of the area of nonperfusion to the total retinal area and increases from *left* to *right*.

Discussion

In this study, we evaluated the correlation between retinal and choriocapillaris microvascular changes on OCTA and disease severity in eyes with DR. In the uncorrected Spearman and Pearson correlations, all OCTA parameters, except one (AFI in the SCP in the Pearson correlation), were correlated statistically significantly with DR severity (Table 2). The DCP vessel density showed the strongest correlation with DR severity, fitting with previous studies that emphasized the important role of the DCP in DR.[13,22,23] Sex and age recently have been shown to influence retinal vascular density as well as FAZ size.[24–27] When we adjusted for hypertension, age, sex, and the correlation between the two eyes of the same participant, the correlations remained significant when DR severity groups were defined as a continuous variable (Table 3).

Table 3. Mixed Effects Models Showing Correlation Between OCTA Parameters and Severity of DR

Outcome Measure	Group, Defined as Continuous Variable		DM Without DR Compared to Healthy		NPDR Compared to Healthy		PDR Compared to Healthy	
	Estimate	*P* Value	Estimate	*P* Value	Estimate	*P* Value	Estimate	*P* Value
FAZ								
SCP	6.460 e^{-02}	2.86 e^{-05}*	5.159 e^{-02}	0.2924	1.148 e^{-01}†	0.0120†	1.948 e^{-01}†	7.14 e^{-05}*
Full retina	7.018 e^{-02}	4.13 e^{-06}*	4.407 e^{-02}	0.3558	7.411 e^{-02}	0.0930	2.270 e^{-01}*	2.80 e^{-06}*
Vessel density								
SCP	−3.563*	<2 e^{-16}*	−1.043	0.3128	−6.832*	9.33 e^{-11}*	−9.941*	<2 e^{-16}*
DCP	−3.718*	<2 e^{-16}*	−1.748	0.0662	−7.086*	7.05 e^{-13}*	−10.608*	<2 e^{-16}*
Full retina	−3.579*	<2 e^{-16}*	−0.437	0.6857	−6.353*	4.33 e^{-09}*	−10.010*	4.44 e^{-16}*
PAN								
SCP	4.613*	<2 e^{-16}*	3.654†	0.0181†	9.125*	2.70 e^{-09}*	13.544*	3.77 e^{-15}*
DCP	5.051*	<2 e^{-16}*	2.556	0.1058	8.247*	1.11 e^{-07}*	15.015*	<2 e^{-16}*
Full retina	3.966*	<2 e^{-16}*	2.866†	0.0268†	6.938*	4.13 e^{-08}*	11.888*	4.44 e^{-16}*
CC	0.549*	9.22 e^{-08}*	0.875*	0.0055*	0.858*	0.0032*	1.856*	1.23 e^{-08}*
Adjusted flow index								
SCP	−4.797 e^{-03}	0.0544	1.557 e^{-02}†	0.0485†	−2.251 e^{-03}	0.7548	−1.054 e^{-02}	0.1678
DCP	−1.566 e^{-02}†	1.08 e^{-07}*	6.756 e^{-03}	0.4376	−2.933 e^{-02}*	0.0004*	−4.014 e^{-02}*	6.05 e^{-06}*
Full retina	−7.013e^{-03}*	0.0079*	1.505 e^{-02}	0.0680	−8.518 e^{-03}	0.2601	−1.578 e^{-02}†	0.0491†
CC	−5.627 e^{-03}*	0.0034*	1.579 e^{-03}	0.7982	−9.479 e^{-03}	0.0978	−1.507 e^{-02}†	0.0130†

* Correlation is significant at the 0.01 level (2-tailed).
† Correlation is significant at the 0.05 level (2-tailed).

Investigative Ophthalmology & Visual Science

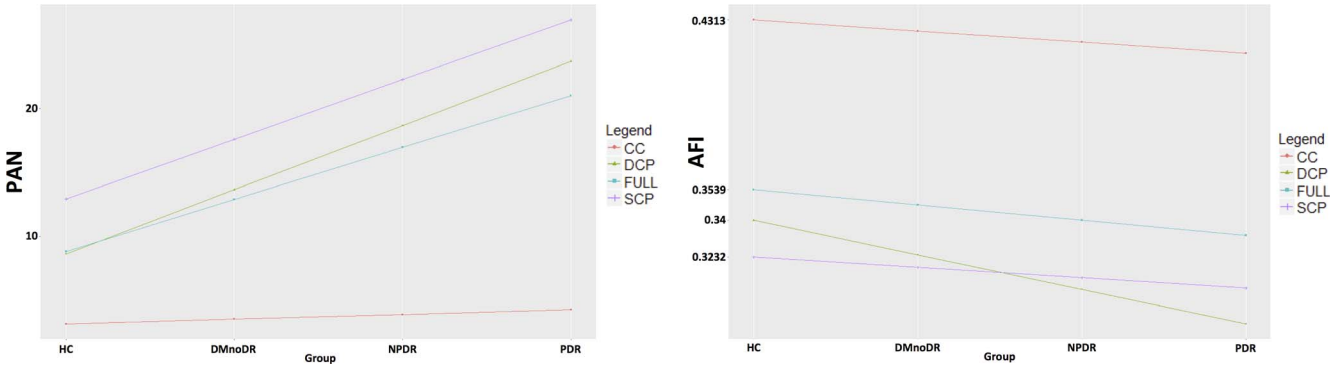

FIGURE 4. Fitted regression lines for PAN and AFI. The fitted regression line for PAN (*left*) measured in the choriocapillaris deviated significantly from the other lines (measured for the superficial and deep capillary plexus and full retina). The fitted regression line for the AFI (*right*) measured in the deep capillary plexus significantly deviated from the other lines (measured for the choriocapillaris, superficial capillary plexus and full retina). CC, choriocapillaris; FULL, full retinal thickness.

When DR severity groups (defined as categorical variables) were compared to healthy controls in the mixed effects model, we observed a difference between DM without DR and healthy controls in PAN measured in the SCP, full retina, and choriocapillaris as well as in the AFI measured for the SCP (Table 3). These results fit well the results of a recent publication by De Carlo et al.,[28] who showed that retinal capillary nonperfusion occurs more frequently in eyes of patients with DM without DR than in eyes of healthy individuals. They also showed that the FAZ is significantly enlarged in eyes of patients with DM without DR compared to healthy eyes, which we did not observe in our study population. The outcomes of their study, however, were based on qualitative evaluation of microvascular changes, as opposed to the quantitative evaluation with correction for covariates as performed in our study.

Dimitrova et al.[29] recently observed a significant difference in vessel density (SCP and DCP) and FAZ area (SCP) comparing healthy controls to eyes of patients with DM without DR. These results differ from ours, however, which could be related to the difference in demographics or lack of correction for covariates in the previous study.

Surprisingly, the AFI in the SCP was significantly higher in the DM without DR group than in the healthy controls, whereas in the NPDR and PDR groups it was lower than in the healthy control group (Table 3). Although the DCP and full retina also had greater AFI in the DM without DR group compared to healthy controls (Table 2), only the SCP AFI remained significant in the adjusted mixed effects model with DR severity considered a categorical variable (Table 3). This finding still was seen after correcting for hypertension in the mixed effects model, and in fact, the full retinal AFI also was significantly higher in the DM without DR in that model. This initial increase followed by subsequent decrease of the SCP AFI with increasing DR severity may explain the lack of a significant linear correlation for AFI in the SCP with increasing DR severity (when disease severity is considered a continuous variable; Table 3). Finding a similar trend after adjusting for hypertension provides further support for higher AFI in DM without DR compared to healthy subjects, a finding that deserves further study as a potential early biomarker of DR before clinically evident retinopathy.

It is important to note that we calculated the AFI for pixels with brightness above a certain threshold and not for the whole en face image. Using this method, signal intensity within vessels served as a surrogate for flow velocity.[30] The AFI is dependent on the average decorrelation values, expressed as pixel brightness in en face OCTA imaging. Decorrelation values and blood flow velocity, however, are correlated linearly only within a limited range, which may explain the mild correlation we found in our study.[30] It has been reported previously that in early stages of diabetes retinal blood flow may be increased before the onset of DR.[31–34] In later stages of DR, a decrease in blood flow has been reported in the literature, which fits well with the decreasing mean AFI values with increasing DR severity observed in our study (Table 2).[31] Based on these previous reports and the adjusted mixed effects model in our study, we hypothesized that higher flow in the SCP (and the full retina) may be an early sign of diabetic changes in eyes without clinical signs of DR. This hypothesis, however, must be explored further in future studies.

Interestingly, the fitted regression line for the AFI at the DCP deviated significantly from the other capillaries, showing a steeper decrease with increasing DR severity (Fig. 4). These findings suggest one of two possibilities: capillaries in the DCP, suffering an early loss of pericytes and subsequent reduction of blood flow,[35] may show a faster decline in blood flow than other networks, or alternatively the AFI may be a more sensitive marker of DR changes than vascular density at the DCP. This decreased flow in the DCP may be an important topic for future studies exploring visual function in DR, as we have demonstrated recently a significant impact of DCP nonperfusion on the integrity of the photoreceptors.[36,37]

We introduced PAN as a new OCTA parameter, which, in its essence, is an inverse approach to vessel density and serves as a quantitative marker for the nonflow area in OCTA.[21] Quantification of nonperfused areas (i.e., nonflow area) has been shown to be sensitive to early capillary closure in DR.[15,38] Furthermore, since there was no vessel density algorithm for the choriocapillaris in the AngioVue software, calculating PAN allowed us to quantify choriocapillaris nonperfusion. The correlation coefficients between DR severity and either vessel density or PAN were very similar in our study (Table 2). However, while vessel density was not significantly different between the DM without DR group and healthy controls, PAN measured in the SCP, full retina, and choriocapillaris was increased significantly in the DM without DR group compared to healthy eyes (Table 3). These results indicated that PAN may be a more sensitive marker for microvascular impairment than vessel density when patient age, sex, and correlation between right and left eyes are considered. The fitted regression line for choriocapillaris PAN deviated significantly from the SCP, DCP, and full retinal regression lines (Fig. 4). This may indicate differential involvement of the retinal and choriocapillaris vasculature in DR with retinal vasculature being correlated more closely with clinical DR severity. Although the concept of diabetic choroidopathy is well established, the role of the choriocapillaris in DR still is incompletely understood.[31,39–42]

Investigative Ophthalmology & Visual Science

In contrast to recent studies showing significant differences in FAZ area between healthy eyes and eyes of patients with DM without DR, we did not observe a significant difference in FAZ measured either in the SCP or in the full retina.[28,29] This may be explained by the high variability of the FAZ area in healthy individuals as well as the correction for covariates in our statistical model.[14,43,44]

Limitations of this study included the retrospective study design and the limited field of OCTA imaging. The issue of trading field of view for better image quality has been addressed as a major shortcoming of current OCTA devices and future studies using OCTA devices with a wider field of view are warranted.[13] Another limitation is that the automated preset algorithm in the AngioVue system only segments two retinal capillary plexuses: the SCP and the DCP. Ours and other groups recently showed that the middle capillary plexus (MCP), which is partly incorporated in the SCP and DCP in the current algorithm, is qualitatively and quantitatively distinct from the SCP and DCP.[6,15,45] As shown in these previous studies, the SCP, MCP and DCP showed different areas of nonperfusion in eyes with DR.[6] Therefore, segmentation of the SCP, MCP, and DCP and quantitative analysis of each individual plexus may yield different outcomes from those found in our study and should be assessed further in future studies. Another limitation of this study is the inclusion of eyes previously treated for DR (15% of the NPDR and 77% of the PDR groups). The vasculature in previously-treated eyes may not reflect the natural course of the disease, given the largely unknown impact of treatment on OCTA parameters. Therefore, additional studies are warranted that focus on treatment-naïve eyes. Finally, we used a spectral-domain optical coherence tomography–based system in our study, which has a limited penetration depth. This may have influenced the evaluation of the choriocapillaris. Strengths of our study included a large study cohort as well as use of statistical models that corrected for covariates.

In conclusion, our study showed that retinal capillary nonperfusion in OCTA is correlated significantly and linearly with disease severity in eyes with DR. Similar to previous studies, we found a strong correlation between DR severity and nonperfusion of the retinal capillary plexuses as well as the choriocapillaris. We introduced PAN as a marker of nonperfusion and showed that it may be used as an imaging biomarker to differentiate healthy eyes from eyes of patients with DM without DR independent of age, sex, or correlation between eyes of the same individual. Furthermore, increased AFI in the SCP, a surrogate for blood flow velocity, may serve as an early indicator for subclinical stages of DR. Finally, the significant decline of AFI (blood flow) in the DCP with increasing DR severity suggested specific flow alterations at this retinal capillary layer that may have functional consequences for photoreceptors and warrant further investigation.[36,37]

Acknowledgments

Supported by Research to Prevent Blindness (unrestricted funds to the Department of Ophthalmology, Northwestern University, Feinberg School of Medicine). Research instrument support was provided by Optovue, Inc., Fremont, California, United States. Supported in part by National Institutes of Health DP3DK108248 (AAF).

Disclosure: **P.L. Nesper**, None; **P.K. Roberts**, None; **A.C. Onishi**, None; **H. Chai**, None; **L. Liu**, None; **L.M. Jampol**, None; **A.A. Fawzi**, None

References

1. Cogan DG, Toussaint D, Kuwabara T. Retinal vascular patterns: IV. Diabetic retinopathy. *Arch Ophthalmol*. 1961; 66:366–378.
2. Hammes H-P, Feng Y, Pfister F, Brownlee M. Diabetic retinopathy: targeting vasoregression. *Diabetes*. 2011;60:9–16.
3. Ashton N. Studies of the retinal capillaries in relation to diabetic and other retinopathies. *Br J Ophthalmol*. 1963;47: 521.
4. Antonetti DA, Klein R, Gardner TW. Diabetic retinopathy. *N Engl J Med*. 2012;366:1227–1239.
5. Garner A. Histopathology of diabetic retinopathy in man. *Eye*. 1993;7:250–253.
6. Park JJ, Soetikno BT, Fawzi AA. Characterization of the middle capillary plexus using optical coherence tomography angiography in healthy and diabetic eyes. *Retina*. 2016;36:2039–2050.
7. Hasegawa N, Nozaki M, Takase N, Yoshida M, Ogura Y. New insights into microaneurysms in the deep capillary plexus detected by optical coherence tomography angiography in diabetic macular edema. *Invest Ophthalmol Vis Sci*. 2016;57: 348–355.
8. Freiberg FJ, Pfau M, Wons J, Wirth MA, Becker MD, Michels S. Optical coherence tomography angiography of the foveal avascular zone in diabetic retinopathy. *Graefes Arch Clin Exp Ophthalmol*. 2016;254:1051–1058.
9. Couturier A, Mané V, Bonnin S, et al. Capillary plexus anomalies in diabetic retinopathy on optical coherence tomography angiography. *Retina*. 2015;35:2384–2391.
10. Ishibazawa A, Nagaoka T, Takahashi A, et al. Optical coherence tomography angiography in diabetic retinopathy: a prospective pilot study. *Am J Ophthalmol*. 2015;160:35–44.
11. Hwang TS, Jia Y, Gao SS, et al. Optical coherence tomography angiography features of diabetic retinopathy. *Retina*. 2015;35: 2371.
12. Kim AY, Chu Z, Shahidzadeh A, Wang RK, Puliafito CA, Kashani AH. Quantifying microvascular density and morphology in diabetic retinopathy using spectral-domain optical coherence tomography angiography. *Invest Ophthalmol Vis Sci*. 2016;57:362–370.
13. Agemy SA, Scripsema NK, Shah CM, et al. Retinal vascular perfusion density mapping using optical coherence tomography angiography in normals and diabetic retinopathy patients. *Retina*. 2015;35:2353–2363.
14. Hwang TS, Gao SS, Liu L, et al. Automated quantification of capillary nonperfusion using optical coherence tomography angiography in diabetic retinopathy. *JAMA Ophthalmol*. 2016; 134:367–373.
15. Zhang M, Hwang TS, Dongye C, Wilson DJ, Huang D, Jia Y. Automated quantification of nonperfusion in three retinal plexuses using projection-resolved optical coherence tomography angiography in diabetic retinopathy. *Invest Ophthalmol Vis Sci*. 2016;57:5101–5106.
16. Moore J, Bagley S, Ireland G, McLeod D, Boulton ME. Three dimensional analysis of microaneurysms in the human diabetic retina. *J Anat*. 1999;194:89–100.
17. Early Treatment Diabetic Retinopathy Study Research Group. Grading diabetic retinopathy from stereoscopic color fundus photographs—an extension of the modified Airlie House classification: ETDRS report number 10. *Ophthalmology*. 1991;98:786–806.
18. Holladay JT. Proper method for calculating average visual acuity. *J Refract Surg*. 1997;13:388–391.
19. Jia Y, Tan O, Tokayer J, et al. Split-spectrum amplitude-decorrelation angiography with optical coherence tomography. *Opt Express*. 2012;20:4710–4725.
20. Alten F, Heiduschka P, Clemens CR, Eter N. Exploring choriocapillaris under reticular pseudodrusen using OCT-angiography. *Graefes Arch Clin Exp Ophthalmol*. 2016;254: 2165–2173.

21. Nesper PL, Soetikno BT, Fawzi AA. Choriocapillaris nonperfusion is associated with poor visual acuity in eyes with reticular pseudodrusen. *Am J Ophthalmo.l* 2017;174:42–55.
22. Lee J, Moon BG, Cho AR, Yoon YH. Optical coherence tomography angiography of DME and its association with anti-VEGF treatment response. *Ophthalmology*. 2016;123:2368–2375.
23. Yu DY, Cringle SJ, Su EN, Yu PK, Jerums G, Cooper ME. Pathogenesis and intervention strategies in diabetic retinopathy. *Clin Exp Ophthalmol*. 2001;29:164–166.
24. Yu J, Jiang C, Wang X, et al. Macular perfusion in healthy Chinese: an optical coherence tomography angiogram study. *Invest Ophthalmol Vis Sci*. 2015;56:3212–3217.
25. Iafe NA, Phasukkijwatana N, Chen X, Sarraf D. Retinal capillary density and foveal avascular zone area are age-dependent: quantitative analysis using optical coherence tomography angiography. *Invest Ophthalmol Vis Sci*. 2016; 57:5780–5787.
26. Coscas F, Sellam A, Glacet-Bernard A, et al. Normative data for vascular density in superficial and deep capillary plexuses of healthy adults assessed by optical coherence tomography angiography. *Invest Ophthalmol Vis Sci*. 2016;57:211–223.
27. Tan CS, Lim LW, Chow VS, et al. Optical coherence tomography angiography evaluation of the parafoveal vasculature and its relationship with ocular factors. *Invest Ophthalmol Vis Sci*. 2016;57:224–234.
28. de Carlo TE, Chin AT, Bonini Filho MA, et al. Detection of microvascular changes in eyes of patients with diabetes but not clinical diabetic retinopathy using optical coherence tomography angiography. *Retina*. 2015;35:2364–2370.
29. Dimitrova G, Chihara E, Takahashi H, Amano H, Okazaki K. Quantitative retinal optical coherence tomography angiography in patients with diabetes without diabetic retinopathy. *Invest Ophthalmol Vis Sci*. 2017;58:190–196.
30. Tokayer J, Jia Y, Dhalla AH, Huang D. Blood flow velocity quantification using split-spectrum amplitude-decorrelation angiography with optical coherence tomography. *Biomed Opt Express*. 2013;4:1909–1924.
31. Pemp B, Schmetterer L. Ocular blood flow in diabetes and age-related macular degeneration. *Can J Ophthalmol*. 2008; 43:295–301.
32. Alder VA, Su EN, Yu DY, Cringle SJ, Yu PK. Diabetic retinopathy: early functional changes. *Clin Exp Pharmacol Physiol*. 1997;24:785–788.
33. Grunwald JE, DuPont J, Riva CE. Retinal haemodynamics in patients with early diabetes mellitus. *Br J Ophthalmol*. 1996; 80:327–331.
34. Kohner EM, Hamilton AM, Saunders SJ, Sutcliffe BA, Bulpitt CJ. The retinal blood flow in diabetes. *Diabetologia*. 1975;11: 27–33.
35. Kur J, Newman EA, Chan-Ling T. Cellular and physiological mechanisms underlying blood flow regulation in the retina and choroid in health and disease. *Prog Retin Eye Res*. 2012; 31:377–406.
36. Scarinci F, Nesper PL, Fawzi AA. Deep retinal capillary nonperfusion is associated with photoreceptor disruption in diabetic macular ischemia. *Am J Ophthalmol*. 2016;168:129–138.
37. Nesper PL, Scarinci F, Fawzi AA. Adaptive optics reveals photoreceptor abnormalities in diabetic macular ischemia. *PLoS One*. 2017;12:e0169926.
38. Schottenhamml J, Moult EM, Ploner S, et al. An automatic, intercapillary area-based algorithm for quantifying diabetes-related capillary dropout using optical coherence tomography angiography. *Retina*. 2016;36:S93–S101.
39. Choi W, Waheed NK, Moult EM, et al. Ultrahigh speed swept source optical coherence tomography angiography of retinal and choriocapillaris alterations in diabetic patients with and without retinopathy. *Retina*. 2017;37:11–21.
40. Cao J, McLeod S, Merges CA, Lutty GA. Choriocapillaris degeneration and related pathologic changes in human diabetic eyes. *Arch Ophthalmol*. 1998;116:589–597.
41. Lutty GA. Effects of diabetes on the eye. *Invest Ophthalmol Vis Sci*. 2013;54:81–87.
42. Hua R, Liu L, Wang X, Chen L. Imaging evidence of diabetic choroidopathy in vivo: angiographic pathoanatomy and choroidal-enhanced depth imaging. *PLoS One*. 2013;8: e83494.
43. Shahlaee A, Samara WA, Hsu J, et al. In vivo assessment of macular vascular density in healthy human eyes using optical coherence tomography angiography. *Am J Ophthalmol*. 2016; 165:39–46.
44. Samara WA, Say EA, Khoo CT, et al. Correlation of foveal avascular zone size with foveal morphology in normal eyes using optical coherence tomography angiography. *Retina*. 2015;35:2188–2195.
45. Hwang TS, Zhang M, Bhavsar K, et al. Visualization of 3 distinct retinal plexuses by projection-resolved optical coherence tomography angiography in diabetic retinopathy. *JAMA Ophthalmol*. 2016;134:1411–1419.

Investigative Ophthalmology & Visual Science